GEODETIC DATA ASSIMILATION FOR EVALUATING VOLCANIC UNREST

Patricia M. Gregg (1), John A. Albright (1), Yan Zhan (1), and J. Cory Pettijohn (1)

(1) Department of Geology, University of Illinois at Urbana-Champaign, Urbana, IL, USA

ABSTRACT

Ensemble based data assimilation approaches, such as the Ensemble Kalman Filter (EnKF), have been widely and successfully implemented to combine observations with dynamic forecast models. In this study the EnKF is adapted to assimilate ground deformation observations from interferometric synthetic-aperture radar (InSAR) and GPS into thermomechanical finite element models (FEM) to evaluate volcanic unrest. Two eruption hindcasts are investigated: the 2008 eruption of Okmok volcano, Alaska and the 2018 eruption of Sierra Negra volcano, Galápagos, Ecuador. At Okmok, EnKF forecasts tensile failure and the lateral movement of the magma from a central pressure source in the lead up to its 2008 eruption indicating potential for diking. Alternatively, at Sierra Negra, the EnKF forecasts significant shear failure coincident with a Mw 5.4 earthquake that preceded the 2018 eruption. These successful hindcasts highlight the flexibility and potential of the volcano EnKF approach for near real time monitoring and hazard assessment at active volcanoes worldwide.

Index Terms— InSAR, GPS, EnKF, FEM, volcano data assimilation

1. INTRODUCTION

Approximately 500 million people live on or near active volcanoes worldwide. The successful mitigation of volcanic disasters for these populations requires the detection of early unrest, an accurate assessment of the precursory signals through modeling, and the efficient and robust communication of potential hazards and risks. Monitoring observations from geophysical campaigns, satellites, and continuous on-the-ground stations can provide early warning, sometimes years in advance of volcanic eruption [1, 2]. However, synthesizing data into dynamic models of an evolving volcanic system poses a great challenge for the volcano hazards community.

While fields such as climate change research, physical oceanography, and hydrologic modeling have made significant advancements in model-data fusion and forecasting techniques in the past decades [3], the field of volcano hazards is in the initial stages of embracing such advances [4-11]. Given the current state of volcano monitoring, significant advancements in multiphysics finite element modeling, and newly adapted approaches in

statistical data assimilation, the field of volcanology is in an ideal position to make rapid advancement in data assimilation and forecasting.

Utilizing the EnKF approach, geodetic ground deformation data are assimilated into multiphysics finite elements models (FEMs) to track the evolution of the magmatic system through time. By using an FEM approach to track stress and strain in the host rock surrounding the magma system, eruption precursors and critical stress states can be evaluated at each time step to assess magma system stability. In this study, we highlight recent EnKF hindcasts of the 2008 eruption of Okmok Volcano, Alaska [4] and the 2018 eruption of Sierra Negra Volcano, Galápagos, Ecuador [11]. For each volcano target we find unique triggering mechanisms and eruption precursors indicating the potential of the EnKF approach for future volcano investigations.

2. NUMERICAL APPROACH

2.1. Thermomechanical Finite Element Method

Our numerical experiments build upon previous finite element model (FEM) developments [12, 13]. We utilize COMSOL Multiphysics 5.3 to implement 2D and 3D, temperature dependent, elastic FEMs for an inflating magma reservoir. COMSOL solves for temperature, and stress and strain in response to applied loads. We are particularly interested in the impact of the thermal structure on the elastic properties of the host rock and the resultant model predictions [12, 14, 15]. As such, we have incorporated a temperature and depth-dependent Young's modulus [15].

Constraining failure in the host rock surrounding a reservoir is critical for determining the stability of the system and the potential for eruption [12, 14-17]. We use a combination of three approaches to evaluate magma chamber stability. First, we investigate faulting in the brittle portions of the model space using a Mohr-Coulomb failure criterion. Second, we investigate the evolution of tensile stresses along the magma chamber boundary. Third, overpressurization of the magma chamber is tracked to determine whether a critical threshold has been reached [18].

2.2. Volcano EnKF

We have adapted the Ensemble Kalman Filter (EnKF), an ensemble-based Markov chain Monte Carlo (MCMC), sequential data assimilation approach, to assimilate large geospatial data into multiphysics FEMs [7]. The EnKF workflow has been adapted for High Performance Computing

(HPC) utilizing a handshake between Python and COMSOL Multiphysics [10]. The HPC volcano EnKF approach, vEnKF, is highly scalable. Individual FEMs are distributed across compute nodes for swift, simultaneous calculation at each time step. A Monte Carlo suite produces the initial vEnKF ensemble with N models. The models are distributed across CPU's and calculated to produce a forecast ensemble. A. In this investigation we use finite element models of a deforming magma chamber. Model outputs include stress and strain, which provide predictions of surface deformation and failure. Data, **D**, include any observations that inform the model (e.g., ground deformation, gravity or mass change, heat flux, seismicity). In this investigation, we have limited our assimilation approach to GPS and InSAR ground deformation data. Measurements and models are combined in the EnKF analysis step to provide the analysis ensemble, A^a :

$$A^{a} = A + XH^{T}(HXH^{T} + C_{d})^{-1}(D - HA),$$

where X is the ensemble covariance matrix, C_d is the measurement covariance matrix, and H is the model operator matrix.

3. OKMOK, ALASKA 2008 ERUPTION

Located on the northern half of Umnak island Alaska, Okmok is a broad shield volcano with a central caldera filled containing several secondary cones that have hosted much of its recent activity. On July 12, 2008, Okmok began to explosively erupt in a prolonged event lasting 5 weeks [19-22]. While the previous eruption in 1997 was predominantly effusive, the 2008 eruption was phreatomagmatic, powered by both the eruption of new lava as well as steam explosions. The eruption reached a VEI of 4 and the ash cloud is believed to have reached approximately 16 km into the atmosphere, disrupting air traffic across the northern Pacific. Given its relative size, this 2008 eruption was notable for the lack of a clear precursory signal. Although the island was well-instrumented, ground inflation had been steady since the start of 2008 with very little precursory seismicity.

The EnKF hindcast of Okmok's 2008 eruption provides a unique view of the system's evolution in the months preceding the event. In particular, while no Mohr-Coulomb failure is forecasted in the lead up to the eruption, an increased number of models experience tensile failure in the weeks prior to the eruption (Figure 1). At the beginning of 2008 there is a marked shift in the trajectory of tensile failure along the reservoir (Figure 1B) and a higher percentage of models in tensile failure (Figure 1A). Additionally, the location of the forecasted tensile failure, along the edge of the pressure source, coincides with location of the eruptive vent near Cone D (Figure 1C). An important finding from this work is that the EnKF is able to capture the changing state of the Okmok system. Had a near real-time approach been implemented in 2008, monitors would have been alerted to the variations in the system state and an increase in eruption potential weeks prior to the explosive event.

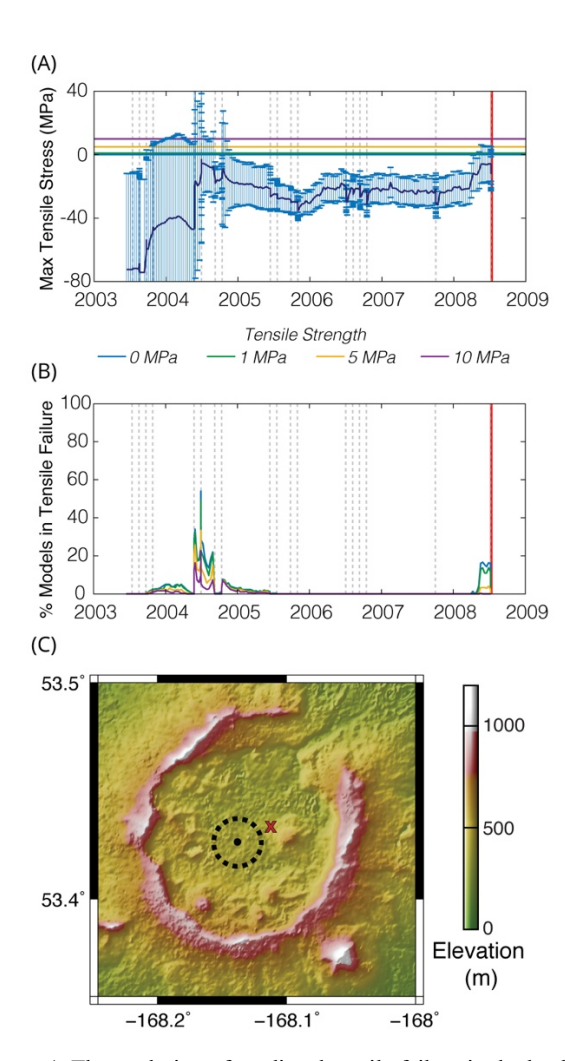
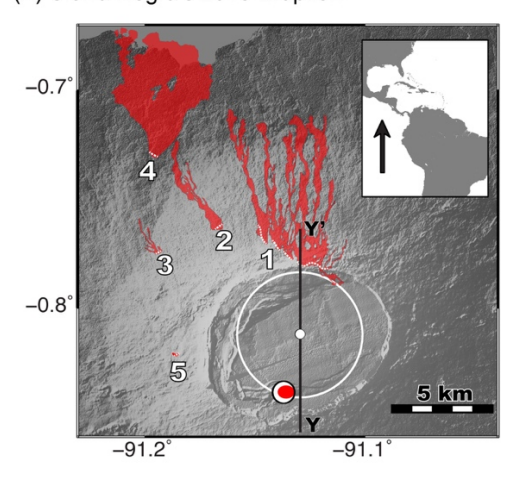


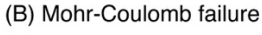
Figure 1. The evolution of predicted tensile failure in the lead up to the 2008 eruption of Okmok [4). (A) Maximum tensile stress calculated along the reservoir wall by EnKF assimilation at each time step. Solid line indicates ensemble mean with 2σ error bars. Horizontal lines indicate threshold tensile strengths. Each time step coincides with the assimilation of either GPS or InSAR data (denoted by vertical, gray dashed lines). (B) Percentage of ensemble members in tensile failure at each time step for four different tensile strengths. (C) Map view of Okmok Caldera showing the center (dot) and extent (dotted line) of the forecasted pressure source (black) relative to the primary vent of the 2008 eruption (red X).

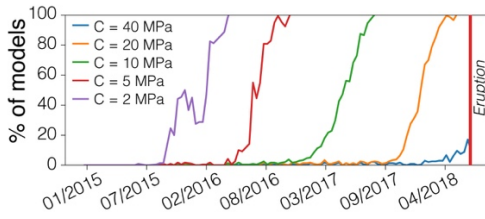
4. SIERRA NEGRA, GALÁPAGOS 2018 ERUPTION

Sierra Negra is a 60x40 km basaltic shield volcano that occupies most of the southern portion of Isabela Island, Ecuador and is the most voluminous of the Galápagos volcanoes [23]. Prior to the previous, 2005 eruption of Sierra Negra, substantial deformation > 5 m was observed, culminating in a M_w 5.4 earthquake and an explosive eruption on 22 October 2005 with a 13-14 km high volcanic plume [24, 25]. Reinflation of Sierra Negra commenced almost immediately following the 2005 eruption, and by the end of 2017, the magnitude of inflation had reached levels

(A) Sierra Negra's 2018 Eruption







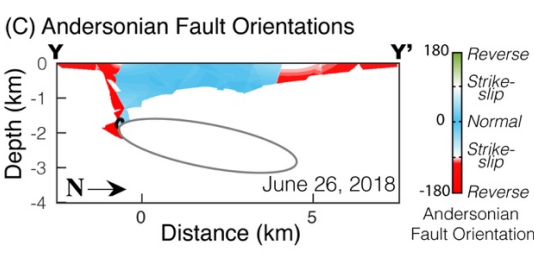


Figure 2. (A) The 2018 eruption of Sierra Negra commenced on June 26 at 1340 LT from five fissures (white dashed lines) with resultant lava flows indicated by red shaded regions [28]. White circle indicates the center of the hindcast source, its extent outlined by the white line. Black line indicates the cross section, Y-Y', illustrated in (C). Focal mechanism solution is shown for the Mw 5.4 earthquake that struck 10 hours prior to the eruption. (B) The percentage of models in the vEnKF ensemble experiencing Mohr-Coulomb failure for a given cohesion, C. (C) Cross section through the center of the mean vEnKF model. Colors represent calculated Andersonian fault orientations [29] in regions of predicted Mohr-Coulomb failure, C = 5 MPa. Black outline indicates region of calculated tensile failure, tensile strength = 1MPa.

comparable to those recorded just prior to the 2005 eruption. The 26 June 2018 eruption (Figure 2A), which commenced at 1340 LT, was preceded by a rapid increase in seismicity including a Mw 5.4 event on the southern side of the caldera that struck at 0315 LT [26-28].

A vEnKF hindcast for Sierra Negra was implemented utilizing Sentinel-1 ascending and descending tracks and a 3D thermomechanical FEM. Calculations of overpressure remained modest throughout the precursory deformation period (< 10 MPa). However, the excessive uplift resulted in

vEnKF predictions of increased brittle failure in the model space for indicating the increasing likelihood of seismicity. Model calculations assuming a cohesion, C = 20 MPa coincide well with an intensification in recorded seismicity in the summer of 2017 [28]. Additionally, calculations of Andersonian fault orientations [29] in regions of predicted Mohr-Coulomb failure, correspond well with the observed spatial extent of seismicity as well as derived focal mechanism solutions [30]. Although the vEnKF forecasts significant Mohr-Coulomb failure in the roof above the reservoir, little to no tensile failure is predicted along the reservoir boundary and no tensile failure is predicted along the northern boundary of the magma reservoir where fissure opened during the 2018 eruption (Figure 2A). In the hours prior to the eruption through-going failure of the host rock is forecasted with the potential for reverse faulting along the southern intracaldera trapdoor fault (Figure 2C). The forecasted failure correlates both spatially and temporally with the Mw 5.4 earthquake that struck the trapdoor fault system 10 hours prior to the 2018 eruption. Given the lack of tensile failure to the north prior to this event, it is thought that the preceding earthquake may have been the ultimate catalyst of the eruption.

5. CONCLUSIONS

The vEnKF has proven to be a powerful method for investigating the evolution of magma systems in their lead up to eruption. At Okmok, vEnKF forecasts tensile failure and the lateral expansion of the magma pressure source prior to its 2008 eruption. Alternatively, at Sierra Negra, EnKF forecasts significant shear failure coincident with a Mw 5.4 earthquake that preceded the 2018 eruption. These successful hindcasts highlight the flexibility and potential of the volcano EnKF approach for near real time monitoring and hazard assessment at active volcanoes worldwide.

Acknowledgements. The authors thank our esteemed data colleagues and partners: Z. Lu, J. Freymeuller, F. Amelung, P. Mothes, S. Koric, D. Geist, and Z. Yunjun. The development of an HPC data assimilation framework for forecasting volcanic unrest is supported by grants from the U.S. National Science Foundation (OCE 1834843, EAR 1752477 – Gregg), NASA (13-ESI13-0034, 80-NSSC19K-0357 – Gregg), National Center for Supercomputing Applications Faculty Fellowship (Gregg), NASA Earth and Space Science Fellowship (Zhan), U.S. National Science Foundation Graduate Research Fellowship (Albright). This research is part of the Blue Waters sustained-petascale computing project, which is supported by the National Science Foundation (OCI-0725070 and ACI-1238993) and the state of Illinois. Blue Waters is a joint effort of the University of Illinois at Urbana-Champaign and its National Center for Supercomputing Applications.

6. REFERENCES

[1] J. Biggs and M. E. Pritchard, "Global Volcano Monitoring: What Does It Mean When Volcanoes Deform?," *Elements,* vol. 13, no. 1, pp. 17-22, Feb 2017.

- [2] E. Chaussard and F. Amelung, "Precursory inflation of shallow magma reservoirs at west Sunda volcanoes detected by InSAR," *Geophysical Research Letters*, vol. 39, Nov 2012.
- [3] G. Evensen, "The Ensemble Kalman Filter: theoretical formulation and practical implementation," *Ocean Dynamics*, vol. 53, pp. 343-367, 16 December 2002 2003.
- [4] J. A. Albright, P. M. Gregg, Z. Lu, and J. Freymueller, "Hindcasting magma reservoir stability preceding the 2008 eruption of Okmok, Alaska," *Geophysical Research Letters*, 2019.
- [5] M. G. Bato, V. Pinel, and Y. Yan, "Assimilation of Deformation Data for Eruption Forecasting: Potentiality Assessment Based on Synthetic Cases," (in English), *Frontiers in Earth Science*, Original Research vol. 5, no. 48, 2017-June-28 2017.
- [6] M. G. Bato, V. Pinel, Y. Yan, F. Jouanne, and J. Vandemeulebrouck, "Possible deep connection between volcanic systems evidenced by sequential assimilation of geodetic data," *Scientific Reports*, vol. 8, Aug 2018, Art. no. 11702.
- [7] P. M. Gregg and J. C. Pettijohn, "A multi-data stream assimilation framework for the assessment of volcanic unrest," *Journal of Volcanology and Geothermal Research*, vol. 309, pp. 63-77, 2016.
- [8] Y. Zhan and P. M. Gregg, "Data assimilation strategies for volcano geodesy," *Journal of Volcanology and Geothermal Research*, no. special issue on Volcano Geodesy, 2017.
- [9] Y. Zhan, P. M. Gregg, E. Chaussard, and Y. Aoki, "Sequential Assimilation of Volcanic Monitoring Data to Quantify Eruption Potential: Application to Kerinci Volcano, Sumatra," *Frontiers in Earth Science*, vol. 5, Dec 2017, Art. no. Unsp 108.
- [10] Y. Zhan, P. M. Gregg, H. Le Mevel, C. A. Miller, and C. Cardona, "Integrating Reservoir Dynamics, Crustal Stress, and Geophysical Observations of the Laguna del Maule Magmatic System by FEM Models and Data Assimilation," *Journal of Geophysical Research-Solid Earth*, 2019.
- [11] P. M. Gregg *et al.*, "Forecasting the June 26, 2018 Eruption of Sierra Negra Volcano, Galapagos (Invited)," *AGU Fall Meet. Suppl.*, no. V12A-08, 2019.
- [12] P. M. Gregg, S. L. de Silva, E. B. Grosfils, and J. P. Parmigiani, "Catastrophic caldera-forming eruptions: Thermomechanics and implications for eruption triggering and maximum caldera dimensions on Earth," *Journal of Volcanology and Geothermal Research*, vol. 241-242, pp. 1-12, 2012.
- [13] E. B. Grosfils *et al.*, "Elastic models of magma reservoir mechanics: A key tool for understanding planetary volcanism," in *Volcanism and Tectonism Across the Inner Solar System*, vol. 401, T. Platz, M. Massironi, P. Byrne, and H. Hiesinger, Eds.: Geological Society, London, Special Publications, 2015, pp. 139-158.
- [14] H. E. Cabaniss, P. M. Gregg, and E. B. Grosfils, "The Role of Tectonic Stress in Triggering Large Silicic Caldera Eruptions," *Geophysical Research Letters*, 2018.
- [15] Y. Zhan and P. M. Gregg, "How accurately can we model magma reservoir failure with uncertainties in host-rock rheology?," *Journal of Geophysical Research*, 2019.
- [16] J. A. Albright, P. M. Gregg, Z. Lu, and J. Freymueller, "Hind-casting the 2008 eruption of Okmok, AK using multi-data stream

- statistical data assimilation," *IAVCEI Scientific Assembly*, vol. Portland, OR, 2017.
- [17] E. B. Grosfils, "Magma reservoir failure on the terrestrial planets: Assessing the importance of gravitational loading in simple elastic models," *Journal of Volcanology and Geothermal Research*, vol. 166, no. 2, pp. 47-75, Oct 2007.
- [18] A. M. Rubin, "Propagation of magma-filled cracks," *Annual Review of Earth and Planetary Sciences*, vol. 23, pp. 287-336, 1995.
- [19] K. M. Arnoult *et al.*, "Infrasound observations of the 2008 explosive eruptions of Okmok and Kasatochi volcanoes, Alaska," *Journal of Geophysical Research-Atmospheres*, vol. 115, Oct 2010, Art. no. D00l15.
- [20] J. Biggs, Z. Lu, T. Fournier, and J. T. Freymueller, "Magma flux at Okmok Volcano, Alaska, from a joint inversion of continuous GPS, campaign GPS, and interferometric synthetic aperture radar," *Journal of Geophysical Research-Solid Earth*, vol. 115, Dec 1 2010, Art. no. B12401.
- [21] T. Fournier, J. Freymueller, and P. Cervelli, "Tracking magma volume recovery at Okmok volcano using GPS and an unscented Kalman filter," *Journal of Geophysical Research-Solid Earth*, vol. 114, Feb 2009.
- [22] Z. Lu, D. Dzurisin, J. Biggs, C. Wicks, and S. McNutt, "Ground surface deformation patterns, magma supply, and magma storage at Okmok volcano, Alaska, from InSAR analysis: 1. Intereruption deformation, 1997-2008," *Journal of Geophysical Research-Solid Earth*, Article vol. 115, p. 14, May 2010, Art. no. B00b02.
- [23] R. W. Reynolds and D. J. Geist, "Petrology of lavas from Sierra Negra volcano, Isabela Island, Galapagos archipelago," *Journal of Geophysical Research-Solid Earth,* vol. 100, no. B12, pp. 24537-24553, Dec 10 1995.
- [24] W. W. Chadwick, Jr., D. J. Geist, S. Jonsson, M. Poland, D. J. Johnson, and C. M. Meertens, "A volcano bursting at the seams: Inflation, faulting, and eruption at Sierra Negra volcano, Galapagos," *Geology*, vol. 34, no. 12, pp. 1025-1028, Dec 2006.
- [25] D. J. Geist *et al.*, "The 2005 eruption of Sierra Negra volcano, Galapagos, Ecuador," *Bulletin of Volcanology*, vol. 70, no. 6, pp. 655-673, Apr 2008.
- [26] A. M. Dziewonski, T.-A. Chou, and J. H. Woodhouse, "Determination of earthquake source parameters from waveform data for studies of global and regional seismicity," *Journal of Geophysical Research*, vol. 86, pp. 2825-2852, 1981.
- [27] G. Ekström, M. Nettles, and A. M. Dziewonski, "The global CMT project 2004-2010: Centroid-moment tensors for 13,017 earthquakes," *Physics of the Earth and Planetary Interiors*, vol. 200-201, pp. 1-9, 2012.
- [28] F. Vasconez *et al.*, "The different characteristics of the recent eruptions of Fernandina and Sierra Negra volcanoes (Galápagos, Ecuador," *Volcanica*, vol. 1, no. 2, pp. 127-133, 2018.
- [29] R. W. Simpson, "Quantifying Anderson's fault types," *Journal of Geophysical Research*, vol. 102, no. B8, pp. 17909-17919, 1997.
- [30] A. Bell *et al.*, "Evidence for System Criticality Prior to Eruption at Sierra Negra Caldera, Galapagos Islands," *IUGG General Assembly Abstracts*, pp. IUGG19-1456, 2019.